JCTC Journal of Chemical Theory and Computation

pubs.acs.org/JCTC Article

Modified Interaction-Strength Interpolation Method as an Important Step toward Self-Consistent Calculations

Szymon Śmiga* and Lucian A. Constantin

Cite This: *J. Chem. Theory Comput.* 2020, 16, 4983−4992 Read Online

ACCESS | Metrics & More | Article Recommendations | Supporting Information

ABSTRACT: The modified point charge plus continuum (mPC) model [Constantin, L. A.; *Phys. Rev. B* **2019**, *99*, 085117] solves the important failures of the original counterpart, namely, the divergences when the reduced gradient of the density is large, such as in the tail of the density and in quasi-dimensional density regimes. The mPC allows us to define a modified interaction-strength interpolation (mISI) method inheriting these good features, which are important steps toward the full self-consistent treatment. Here, we provide an assessment of mISI for molecular systems (*i.e.*, considering thermochemistry properties, correlation energies, vertical ionization potentials, and several noncovalent interactions), harmonium atoms, and functional derivatives in the strong-interaction limit. For all our tests, mISI provides a systematic improvement over the original ISI method. Semilocal approximations of the second-order Görling−Levy (GL2) perturbation theory are also considered in the mISI method, showing considerable worsening of the results. Possible further development of mISI is briefly discussed.

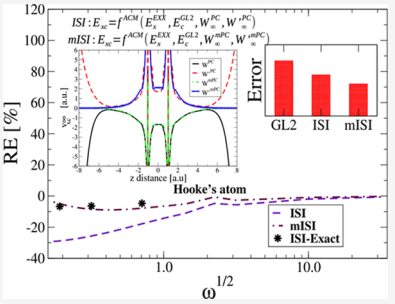

1. INTRODUCTION

The exact exchange−correlation (XC) functional can be formally defined using the adiabatic connection formalism as[1−7]

$$E_{xc}[\rho] = \int_0^1 W_\lambda[\rho]\mathrm{d}\lambda \tag{1}$$

where ρ is the electron density, λ is the electron−electron interaction strength, and

$$W_\lambda[\rho] = \langle \Psi_\lambda[\rho]|\hat{V}^{ee}|\Psi_\lambda[\rho]\rangle - U[\rho] \tag{2}$$

is the density-fixed linear adiabatic connection integrand, with $\Psi_\lambda[\rho]$ being the antisymmetric wave function that minimizes $\hat{T} + \lambda\hat{V}_{ee}$ while yielding the density ρ ($\hat{T}$ and $\hat{V}_{ee}$ are the kinetic and electron−electron interaction operators, respectively), and $U[\rho]$ being the Hartree energy.

Many accurate hybrid XC functionals are based on, and explained by, this method,[4,6,8−10] which provides a rationale for mixing the Hartree−Fock (HF) exchange with semilocal XC functionals.[11] Moreover, the basic Görling−Levy (GL) perturbation theory[12−14] uses a generalized adiabatic connection formula[13] to obtain the Taylor expansion of the correlation energy at a small coupling constant ($\lambda \to 0$). The adiabatic connection formalism also stays behind the more recent and sophisticated double hybrids[15] that are using either the second-order Møller−Plesset[16] (MP2) correlation mixed with fractions of HF exchange and semilocal XC functionals[17−23] into the generalized Kohn−Sham (KS) density functional theory (DFT) scheme[24,25] or GL2 correlation[13] combined with fractions of KS-DFT exact exchange and semilocal XC functionals[26] into the optimized effective potential (OEP) scheme of the true KS-DFT.[26−29] The adiabatic connection is also of utmost importance for the ground-state calculations of linear-response time-dependent DFT, being part of the so-called adiabatic connection fluctuation-dissipation theorem that provides a framework for high-level, orbital-dependent methods based on XC kernel approximations.[30−45]

Here, we focus on the interaction-strength interpolation (ISI) method[46−48] that accurately interpolates the weak ($\lambda \to 0$)- and strong ($\lambda \to \infty$)-interaction limits that are well known. Thus, in the weak-interaction limit, the GL perturbation theory becomes exact[46]

$$W_\lambda[\rho] = W_0[\rho] + W_0'[\rho]\lambda + \cdots \tag{3}$$

where $W_0[\rho] = E_x[\rho]$ is the exact KS-DFT exchange functional and $W_0'[\rho] = 2E_c^{GL2}[\rho]$. On the other hand, the strong-interaction limit is

$$W_\lambda[\rho] = W_\infty[\rho] + W_\infty'[\rho]\lambda^{-1/2} + \cdots \tag{4}$$

where $W_\infty[\rho]$ and $W_\infty'[\rho]$ can be found in the strictly correlated electron (SCE) approach,[49] but in practice, they have been approximated from the second-order gradient

Received: April 2, 2020
Published: June 19, 2020

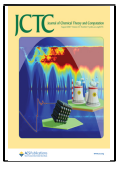

expansion (GE2) of the point charge plus continuum (PC) model.[46−48] Starting from the ISI method, several improvements and variants have been proposed.[49−65] In particular, we mention the methods of refs 49, 50, which remove the spurious λ^{-1} term in the large λ limit of W_λ, keeping the almost same accuracy of the XC energy as the original ISI method. Moreover, correlation energy densities have been constructed from local interpolations along the adiabatic connection curve.[57,62,63,65−67]

Recently, the modified ISI (mISI) method has been developed,[65] which solves important failures of the original ISI approach in the tail of the density and in quasi-low dimensional density regimes. The mISI method has been tested on very few atoms showing improved correlation energies over its initial variant. In this article, we assess mISI for molecular systems, using the OEP exact exchange (OEPx) orbitals and densities. Noting that mISI and ISI are pure KS-DFT functionals and not wave function methods, the choice of OEPx orbitals is the most physical, presumably being very close to the true self-consistent ISI orbitals.

The GL2 correlation energy $E_c^{GL2}[\rho]$ enters the expressions of ISI and mISI functionals, as shown, *e.g.*, in eq 17 of ref 60. Because GL2 depends on all occupied and unoccupied orbitals and orbital energies, its evaluation even with OEPx orbitals is still very expensive. In this sense, semilocal approximations of $E_c^{GL2}[\rho]$ are of interest not only for simplification of the ISI and mISI methods but also for the development of correlation functionals compatible with exact exchange.[68,69] Hence, in our assessment, we also consider the mISI@TPSS-GL2 method that replaces the true GL2 with the TPSS-GL2 meta-generalized-gradient approximation (meta-GGA) correlation functional,[68] which is one of the most accurate GL2 approximations available nowadays (see Table S12 of ref 70 for a comparison of few GL2 models).

This paper is organized as follows: In Section 2, we show a brief theoretical overview of the methods; in Section 3, we report the computational details; and in Section 4, we present and analyze the results. Finally, in Section 5, we summarize our conclusions.

2. THEORETICAL OVERVIEW OF THE METHODS

Both ISI and mISI functionals have the same $W_\lambda[\rho]$ integrand in eq 1

$$W_\lambda[\rho] \approx W_\lambda^{(m)ISI}[\rho] = W_\infty[\rho] + \frac{X[\rho]}{\sqrt{1 + Y[\rho]\lambda} + Z[\rho]} \tag{5}$$

where $X = xy^2/z^2$, $Y = x^2y^2/z^4$, $Z = xy^2/z^3 - 1$, and $x = -4E_c^{GL2}$, $y = W'_\infty$, $z = W_0 - W_\infty$ which, in turn, lead to following XC functional expression

$$E_{xc}^{(m)ISI} = W_\infty + \frac{2X}{Y}\left[\sqrt{1+Y} - 1 - Z\ln\left(\frac{\sqrt{1+Y}+Z}{1+Z}\right)\right] \tag{6}$$

The ISI functional approximates W_∞ with the GE2 of the PC model, and W'_∞ has been fitted to the PKZB meta-GGA[71] counterpart such that

$$W_\infty^{PC}[\rho] = \int d\mathbf{r}\,\{A\rho^{4/3} + B\frac{|\nabla\rho|^2}{\rho^{4/3}}\},$$
$$= \int d\mathbf{r}\, A\rho^{4/3}(1 - 0.14s^2) \tag{7}$$

and

$$W_\infty'^{PC}[\rho] = \int d\mathbf{r}\,\{C\rho^{3/2} + D\frac{|\nabla\rho|^2}{\rho^{7/6}}\},$$
$$= \int d\mathbf{r}\, C\rho^{3/2}(1 - 0.638s^2) \tag{8}$$

where $s = |\nabla\rho|/[2(3\pi^2)^{1/3}\rho^{4/3}]$ is the reduced gradient of the density, $A = -1.451$ and $C = 1.535$ are the LDA low-density-limit coefficients, $B = 0.005317$ is the second-order gradient expansion coefficient of the PC model, and $D = -0.02558$ was fixed from $W_\infty'^{PKZB}[\rho]$ of the He atom.

On the other hand, mISI uses the following expressions[65]

$$W_\infty^{mPC}[\rho] = \int d\mathbf{r}\, A\rho^{4/3}F_\infty(s),$$
$$F_\infty(s) = \frac{1 + as^2}{1 + (a + 0.14)s^2} \tag{9}$$

and

$$W_\infty'^{mPC}[\rho] = \int d\mathbf{r}\, C\rho^{3/2}\frac{1 + bs^2}{1 + s^2} \tag{10}$$

Here, $a = 2$ is the smallest integer that ensures $W_\infty^{mISI}[\rho] \le sLL[\rho]$, where $sLL[\rho] = A\int d\mathbf{r}\,\rho^{4/3} - 0.245\int d\mathbf{r}\,\rho^{4/3}s^{1/4}$ is the simplified gradient-dependent bound of Lewin and Lieb.[72,73] Note that $W_\infty^{mPC}[\rho]$ still recovers the GE2 of the PC model. Finally, $b = 1.3$ has been fitted to the correlation energy of the He atom.

By construction, mISI permits local interpolations along the adiabatic connection[57,62] and the adiabatic connection semi-local correlation (ACSC) functional formalism has been constructed.[65] Thus, for completeness, we will also show results with ACSC GGA correlation functional combined with OEPx.

The ACSC energy per particle $\epsilon_c^{ACSC}(\mathbf{r})$ is defined by $E_c^{ACSC}[\rho] = \int d\mathbf{r}\,\rho\epsilon_c^{ACSC}(\mathbf{r})$, where[65]

$$\rho\epsilon_c^{ACSC}(\mathbf{r}) = \int_0^1 d\lambda\, w_{c,\lambda}(\mathbf{r}) = w_\infty^{mPC}(\mathbf{r}) - w_0(\mathbf{r})$$
$$+\frac{2X(\mathbf{r})}{Y(\mathbf{r})}\left[\sqrt{1+Y(\mathbf{r})} - 1 - Z(\mathbf{r})\ln\left(\frac{\sqrt{1+Y(\mathbf{r})}+Z(\mathbf{r})}{1+Z(\mathbf{r})}\right)\right] \tag{11}$$

while

$$X(\mathbf{r}) = -2w_0'(\mathbf{r})(w'^{mPC}_\infty(\mathbf{r}))^2/(w_0(\mathbf{r}) - w_\infty^{mPC}(\mathbf{r}))^2,$$
$$Y(\mathbf{r}) = 4(w_0'(\mathbf{r}))^2(w'^{mPC}_\infty(\mathbf{r}))^2/(w_0(\mathbf{r}) - w_\infty^{mPC}(\mathbf{r}))^4,$$
$$Z(\mathbf{r}) = -1 - 2w_0'(\mathbf{r})(w'^{mPC}_\infty(\mathbf{r}))^2/(w_0(\mathbf{r}) - w_\infty^{mPC}(\mathbf{r}))^3 \tag{12}$$

Here, all energy densities $w_\lambda(\mathbf{r})$, $w_\lambda'(\mathbf{r})$ are defined by $W_\lambda = \int d\mathbf{r}\, w_\lambda(\mathbf{r})$ and $W_\lambda' = \int d\mathbf{r}\, w_\lambda'(\mathbf{r})$.

The ACSC energy density is a local interpolation along the adiabatic connection, and it is meaningful when all of the energy densities are in the same gauge. Moreover, eq 11 is well

https://dx.doi.org/10.1021/acs.jctc.0c00328
J. Chem. Theory Comput. 2020, 16, 4983−4992

Table 1. Error Statistics (MAE and MARE) of Several Thermochemistry Properties[g]

			@OEPx				
	MP2	OEP2-sc	GL2	ISI[f]	mISI[f]	mISI[e]	ACSC
Correlation Energies (9 Atoms and 27 Molecules)							
MAE[a]	24.4	18.4	95.4	42.3	**34.9**	85.9	73.6
MARE[b]	10.5	8.7	26.6	10.4	**8.3**	21.4	16.9
Atomization Energies (27 Molecules)							
MAE[cI]	5.5	8.0	37.8	16.8	**15.1**	14.8	17.8
MARE[b]	5.2	7.3	31.6	15.2	**13.4**	13.2	17.2
Atomization Energies (AE6 Test)							
MAE[cI]	12.2	17.1	82.1	32.7	**23.6**	25.5	21.0
MARE[b]	3.7	5.6	23.6	13.6	**11.7**	7.5	6.9
Atomization Energies (Small Radicals)							
MAE[cI]	6.1	15.7	53.0	21.7	**16.6**	30.3	34.2
MARE[b]	3.9	12.1	89.1	17.0	**12.2**	31.1	46.4
Kinetics (K9 Test)							
MAE[cI]	2.8	14.9	18.9	16.0	**15.0**	15.9	14.8
MARE[b]	22.5	46.5	75.9	45.5	**37.8**	68.3	68.6
HTR Test							
MAE[cI]	13.5	2.2	25.4	14.8	**12.2**	2.9	2.8
MARE[b]	143.5	32.6	259.5	150.2	**119.0**	29.5	34.0
21 Isomerization Energies (ISO21 Test)							
MAE[cI]	0.89	0.39	20.71	12.48	**10.97**	7.16	6.61
MARE[b]	7.97	16.59	96.60	42.74	**23.87**	82.39	84.89
31 Closed-Shell Reaction Energies							
MAE[cI]	2.0	3.0	10.6	4.7	**4.6**	11.4	10.3
MARE[b]	46.8	34.5	106.3	**54.5**	57.3	144.8	125.7
26 Open-Shell Reaction Energies							
MAE[cI]	4.3	3.4	18.3	11.5	**10.4**	12.2	11.6
MARE[b]	12.3	12.7	51.5	34.6	**29.5**	35.6	30.2
32 Vertical Ionization Potentials (VIP)							
MAE[d]	0.2	0.2	1.2	0.6	**0.5**	0.4	0.4
MARE[b]	2.4	1.2	9.0	4.9	**4.3**	3.8	3.6

[a]In mHa. [b]In %. [c]In kcal/mol. [d]In eV. [e]With TPSS-GL2. [f]Corrected for size-consistency error (see ref 61). [g]The best result between ISI and mISI of each line is highlighted in bold style. The full results of all tests are reported in ref 70. The OEP2-sc results are fully self-consistent, the MP2 and (reference) CCSD(T) results are calculated on top of HF orbitals, and the results of the other methods (GL2, ISI, mISI, mISI@TPSS-GL2, ACSC) are computed on top of OEPx orbitals.

defined only when $w_0(\mathbf{r}) > w_\infty^{\mathrm{mPC}}(\mathbf{r})$,[65] which is violated by the exact exchange energy density in the conventional gauge of the electrostatic potential of the XC hole,[55,74] but it is satisfied by the exact exchange energy density in the TPSS gauge.[65,74] Thus, all energy densities should be in the TPSS gauge, which is more appropriate for semilocal expressions. Because of their semilocal nature, both $w_\infty^{\mathrm{mPC}}(\mathbf{r})$ and $w_\infty'^{\mathrm{mPC}}(\mathbf{r})$ can be considered to be in the TPSS gauge.

For the ACSC GGA correlation functional, we use $w_0'(\mathbf{r}) = 2\rho\epsilon_c^{\mathrm{PBE-GL2}}$ and $w_0(\mathbf{r}) = \rho\epsilon_x^{\mathrm{PBE}}(\mathbf{r})$ as in ref 65, where $\epsilon_c^{\mathrm{PBE-GL2}}$ and $\epsilon_x^{\mathrm{PBE}}$ are the GL2 and exchange energy densities of the popular PBE GGA functional.[65,75]

The nonlinear form of the ISI correlation functional expression leads to the increase of size-consistency error,[58,61] *i.e.*, the total energy of two nonidentical, distant systems is not equal to the sum of energies of subsystems A and B separately, $E_{\mathrm{xc}}^{(\mathrm{m})\mathrm{ISI}}(AB)_{R\to\infty} \neq E_{\mathrm{xc}}^{(\mathrm{m})\mathrm{ISI}}(A) + E_{\mathrm{xc}}^{(\mathrm{m})\mathrm{ISI}}(B)$. As is generally known, the lack of size consistency may lead to wrong predictions, *e.g.*, for atomization or binding energies of molecular systems.[76] This feature can be restored, without additional cost, utilizing the sum over fragments idea from ref 61, which allows us to compute the correlation energies of the infinitely far fragments ($E_{\mathrm{xc}}^{(\mathrm{m})\mathrm{ISI}}(AB)_{R\to\infty}$) utilizing as ingredients in eq 6 the sum of energies of isolated parts. Then, the size-consistency correction can be written (for considered case) as

$$\Delta_{\mathrm{SCC}}^{(\mathrm{m})\mathrm{ISI}} = E_{\mathrm{xc}}^{(\mathrm{m})\mathrm{ISI}}(A) + E_{\mathrm{xc}}^{(\mathrm{m})\mathrm{ISI}}(B) - E_{\mathrm{xc}}^{(\mathrm{m})\mathrm{ISI}}(AB)_{R\to\infty} = \sum_{i=A}^{B} E_{\mathrm{xc}}^{(\mathrm{m})\mathrm{ISI}}(W(\rho_i)) - E_{\mathrm{xc}}^{(\mathrm{m})\mathrm{ISI}}\left(\sum_{i=A}^{B} W(\rho_i)\right) \quad (13)$$

where $W[\rho] = \{E_x[\rho], E_c^{\mathrm{GL2}}[\rho], W_\infty[\rho], W_\infty'[\rho]\}$ is a compact notation for all ISI input ingredients (for more technical details, we refer the reader to ref 61).

3. COMPUTATIONAL DETAILS

All methods considered in the present study have been implemented in a locally modified version of the ACES II[77] program. The ISI, mISI, as well as ACSC and mISI with TPSS-GL2 results have been obtained in a post-self-consistent-field (SCF) manner, using as a reference OEPx SCF converged quantities (*i.e.*, orbitals, orbital energies, and densities). As in our previous studies,[26,29,60,78−81] to solve the OEPx equation, we have employed the finite-basis set procedure of refs 82, 83. To enable the comparison with GL2 results and avoid problems related to full SCF treatment[78−80,84] (see also the

https://dx.doi.org/10.1021/acs.jctc.0c00328
J. Chem. Theory Comput. 2020, 16, 4983−4992

discussion in refs 29, 85, 86), the reported GL2 results are obtained in the same manner. As reference data, we have utilized the coupled-cluster single double and perturbative triple [CCSD(T)][87] results obtained in the same basis set, to make a comparison on the same footing and to reduce basis set-related errors. Additionally, for comparison, we also report the results of the MP2[16] and *ab initio* DFT OEP2-sc methods.[88]

To assess all methods, we have considered several test cases:

- Correlation energies: evaluated for the set of 9 atoms and 27 small closed- and open-shell molecules from refs 81, 89.
- Thermochemistry data: This set contains atomization energies, *i.e.*, AE6,[90,91] G2 subset[89] (see the Supporting Information of ref 81 for more details), small radicals,[92] K9 barrier heights,[91,93] 21 isomerization/reaction energies (ISO21),[76] closed- and open-shell reaction energies listed in refs 81, 94, and the hydrogen transfer reactions (HTR).[81,95] All of the aforementioned calculations have been performed using uncontracted cc-pVTZ basis sets of Dunning[96] without counterpoise corrections for basis set superposition error (BSSE). In the case of atomization energies, the size-consistency correction from ref 61 was employed.
- Vertical ionization potentials: 32 vertical ionization potentials (VIP)[79] computed as the energy difference between the neutral and the ionic species.[97] The computational setup, namely, basis sets and geometries (in the case of molecules), is identical to that in ref 79.
- Noncovalent interactions data: The interaction energies of several types of noncovalent interacting molecular systems also used in our previous studies,[98−101] such as weak interaction (WI), dipole−dipole interaction (DI6), hydrogen-bond interaction (HB6), double-hydrogen-bond interaction (DHB), and charge transfer interaction (CT7). The energies have been obtained using an uncontracted aug-cc-pVTZ[102] basis sets together with the geometries from refs 103−106. All quantities have been calculated without counterpoise corrections for BSSE. In all cases, the size-consistency correction from ref 61 was employed.
- Harmonium atoms: We have performed calculation for various values of ω in the Hooke's atom model[107] ranging between 0.03 (strong interaction) to 1000 (weak interaction) using a even-tempered Gaussian basis set from ref 108 (N = 8, L = 0, 1). The accuracy of full configuration interaction (FCI) results employing this basis set for all values of ω was cross-checked with the exact ones reported in ref 108 yielding, in total, a mean absolute error (MAE) of 0.002 Ha and a mean absolute relative error (MARE) of 0.06%. Because the ISI formula interpolates between weak- and strong-correlation limits, this test seems to be essential for the assessment of XC formula accuracy.
- Potentials for the strong-interaction limit: We have computed the functional derivatives of original and modified PC W_∞ and W'_∞ models in a post-SCF manner using OEPx densities. This approach was already successfully utilized in some studies[60,109−111] to investigate the quality of the potentials.

4. RESULTS

Here, we present and analyze results for thermochemistry, noncovalent interactions, and Hooke's atom[112−115] at various frequencies ω of the harmonic potential. We also investigate the potentials for the strong-interaction limit for a few systems.

4.1. Thermochemistry Results. In Table 1, we present the error statistics (MAE and MARE) of the thermochemistry results. We observe that the mISI method shows a systematic improvement over the ISI method, for all of the tests. On the other hand, GL2 fails badly, being the worst method here. We recall that the GL2[13] correlation energy expression is

$$E_c^{\mathrm{GL}\,2} = -\frac{1}{4}\sum_{abij}\frac{|\langle ij||ab\rangle|^2}{\varepsilon_a+\varepsilon_b-\varepsilon_i-\varepsilon_j} - \sum_{ia}\frac{|\langle i|v_x^{\mathrm{KS}}-\hat{v}_x^{\mathrm{HF}}|a\rangle|^2}{\varepsilon_a-\varepsilon_i} \tag{14}$$

where the indices i, j, a, and b are used for occupied and virtual KS orbitals, ε's are the KS eigenvalues, and v_x^{KS} and $\hat{v}_x^{\mathrm{HF}}$ are the local, multiplicative KS OEPx and the nonlocal HF exchange potentials, respectively. The first term on the right-hand side of eq 14 is the same as the MP2 correlation energy expression, the only difference being computed using KS OEPx orbitals and orbital energies instead of the HF ones. The last term of eq 14 is small[80] in comparison to the first one such that E_c^{GL2} is approximately E_c^{MP2} evaluated with KS orbitals. A comparison between the MP2 and GL2 results of Table 1 shows huge accuracy differences. In this respect, the ISI and mISI methods show significantly improved performance over GL2. This is a consequence of attenuating the GL2 energy term[60,79,80] in the ISI functional expression. Nevertheless, in general, they are still worse than MP2.

On the other hand, mISI@TPSS-GL2, which replaces into the mISI expression the GL2 term with the semilocal TPSS-GL2 variant, is usually worse than mISI, especially for the correlation energies of atoms and molecules. Indeed, more reliable semilocal approximations of GL2 are needed. Finally, the ACSC GGA correlation combined with OEPx exact exchange has a similar accuracy to mISI@TPSS-GL2.

Next, in Figure 1, we show the atomization energy errors versus correlation energy errors for the set of 27 small molecules, used also in Table 1. For almost all of the molecules, the mISI method performs better than the ISI for both properties. We also mention that the worst results are

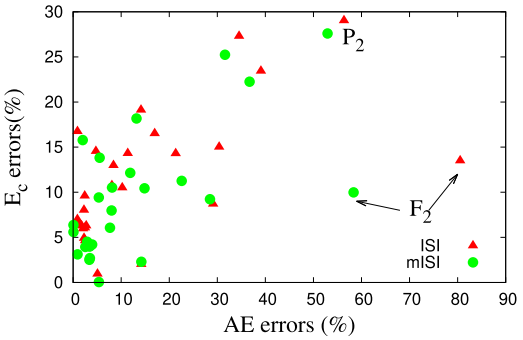

Figure 1. Absolute relative errors (in %) of the atomization energies (AE) versus the ones of the correlation energies, for a set of 27 small molecules BeH, OH, NH_2, NH, NO, PH_2, O_2, S_2, SiH_2, C_2H_5, CH_2, CH_3, CN, COH, CH_4, LiF, Li_2, F_2, CO, CH_2, H_2, CS, LiH, N_2, P_2, NaCl, and H_2O. For the worst cases F_2 and P_2, GL2 fails badly for atomization energies, with errors of 188 and 73%, respectively.

https://dx.doi.org/10.1021/acs.jctc.0c00328
J. Chem. Theory Comput. 2020, 16, 4983−4992

found from F_2 and P_2, which are difficult cases in quantum chemistry, due to their multiconfiguration character.[116]

4.2. Noncovalent Interaction Results. In Figure 2, we report the binding energy curves for three representative cases,

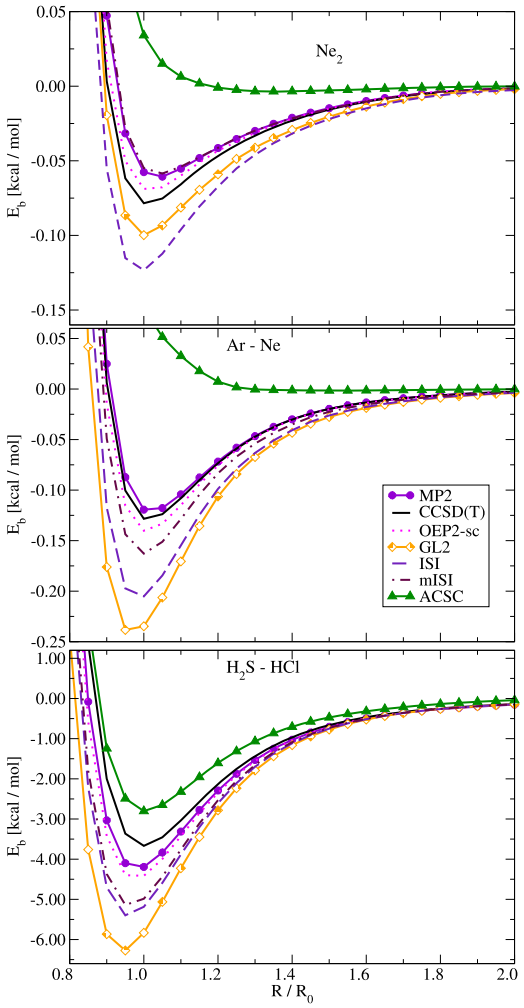

Figure 2. Binding energy curves of Ne_2 (top), Ne−Ar (middle), and H_2S−HCl (bottom) computed using different theoretical methods. In the case of ISI and mISI methods, the size-consistency correction from ref 61 was employed.

namely, Ne_2, Ar−Ne, and H_2S−HCl dimers. In the case of ISI and mISI curves, to enable the comparison with reference results, we have applied the size-consistency correction from ref 61.

First of all, we note that the ACSC gives too shallow binding curves similar to most semilocal functionals. Almost same behavior (not reported) was observed for the mISI@TPSS-GL2 method. The ISI and mISI methods, in turn, reduce the huge overestimation of the GL2 method, with one exception of Ne dimer where ISI gives slightly worse predictions. Nevertheless, also in this case, the utilization of modified point charge plus continuum (mPC) variants of W_∞ and W'_∞ corrects the predictions. The mISI method, in general, performs better than the ISI method, the results being much closer to reference CCSD(T) and to the *ab initio* OEP2-sc data.

This finding is further confirmed by the data gathered in Table 2, where we report the error statistics obtained for several classes of noncovalent interacting molecular systems. The overall statistics confirm previous findings. The mISI outperforms the ISI method, giving in the same time results comparable to the OEP2-sc method. The only exception is for the HB6 test, where we observe an inverse trend. However, a closer look at the total energies (used to calculate HB6 binding energies) shows also here very good performance of the mISI method. The MAEs of total energies, calculated for GL2, ISI, and mISI with respect to the CCSD(T) reference, follow the general observed trend mISI (0.11 Ha) < ISI (0.14 Ha) < GL2 (0.28 Ha). This may indicate that the relatively good performance of ISI for the HB6 binding energies can be related to some error balancing between W_∞^{PC} and W'^{PC}_∞ GE2 terms.

We also note that in the case of WI systems, the ISI and mISI methods yield quite large MAE and MARE. This is caused by large errors given by two dimers, namely, He−Ne and He−Ar. We have found that the large overestimation of ISI binding energies is inherited from the GL2 method, which gives energies of 0.90 and 0.83 kcal/mol for He−Ne and He−Ar, respectively. At the same time, the reference CCSD(T) results yield −0.04 and −0.06 kcal/mol for these two cases. To explain this, we have had a closer look at the GL2 total energies involved in the calculation of the binding energy of the He−Ne dimer. It has turned out that while the Ne and He−Ne dimer total GL2 energies largely overestimate the reference CCSD(T) data (approximately by about 80 mHa), the He total GL2 energy gives quite accurate results, being only 6.4 mHa off CCSD(T) data, in consequence, causing the rise of large error in the binding energy. Nevertheless, we note that both the ISI and mISI methods slightly reduce the value of GL2 binding energies for both dimers.

In Table S13 of ref 70, we report additionally the comparison of binding energies obtained from the ISI and mISI methods using HF reference orbitals. Because the MP2 method already provides quite accurate results (MAE = 0.38 kcal/mol, MARE = 12.58%), the improvement seen in ISI and mISI results, which give here overall MAEs of 0.25 kcal/mol (MARE = 10.26%) and 0.29 kcal/mol (MARE = 17.11%), respectively, is not so significant as observed in Table 2.

To conclude, the mISI shows a systematic improvement over the ISI method, and most importantly, both these methods provide significant correction over GL2, which fails badly, being the worst method for all of the tests.

4.3. Hooke's Atom. Figure 3 reports the errors in the total energies of harmonium atoms calculated for various values of ω ranging between 0.03 and 1000 for several methods. Because both ISI formulas interpolate between weak- and strong-correlation limits, this type of test can be of utmost importance for checking their accuracy and smooth transition between these two regimes. An inspection of the figure reveals that the best performance is given by the mISI method closely followed by ISI, OEP2-sc, and MP2 results. This indicates that the modified GGA PC formula, which fixes the behavior of ISI functional in the density tail, has a strong impact on the proper description of both regimes. In medium- and weakly correlated limits, we observe really good performance of the GL2 method. This is not surprising because GL2 becomes exact in this regime. On the other hand, in the strongly correlated limit, the GL2 method shows the worst performance of all methods. The ACSC and mISI@TPSS-GL2 give similar performance to the *ab initio* OEP2-sc method, namely, a small error for $\omega^{1/2} < 1$ and a large overestimation for larger values of ω.

https://dx.doi.org/10.1021/acs.jctc.0c00328
J. Chem. Theory Comput. 2020, 16, 4983−4992

Table 2. MAE and MARE for Noncovalent Interaction Test Sets[e]

			@OEPx				
	MP2	OEP2-sc	GL2	ISI[d]	mISI[d]	mISI[c]	ACSC
				WI			
MAE[a]	0.04	0.05	0.51	0.36	**0.24**	1.96	0.32
MARE[b]	18.53	17.08	598.63	455.11	**426.50**	899.71	150.26
				HB6			
MAE[a]	0.17	0.27	0.75	**0.39**	0.70	0.64	0.66
MARE[b]	1.81	4.32	9.27	**4.92**	7.28	7.50	6.49
				DI6			
MAE[a]	0.45	0.71	2.16	1.41	**1.14**	1.01	1.09
MARE[b]	12.85	20.24	64.05	42.53	**34.80**	38.97	34.77
				CT7			
MAE[a]	0.55	1.35	2.54	1.71	**1.39**	1.94	1.64
MARE[b]	14.99	40.25	80.36	54.94	**44.61**	69.62	60.33
				DHB			
MAE[a]	0.54	0.85	1.62	0.98	**0.79**	0.91	1.01
MARE[b]	8.19	13.18	30.31	18.52	**15.17**	20.54	20.53
				Overall			
MAE[a]	0.38	0.74	1.63	1.05	**0.91**	1.37	1.03
MARE[b]	12.58	24.28	154.22	113.00	**103.06**	195.24	58.49

[a]In kcal/mol. [b]In %. [c]With TPSS-GL2. [d]Corrected for size-consistency error (see ref 61). [e]The best result between ISI and mISI of each line is highlighted in bold style. The OEP2-sc results are fully self-consistent, the MP2 and (reference) CCSD(T) results are calculated on top of HF orbitals, and the results of the other methods (GL2, ISI, mISI, mISI@TPSS-GL2, ACSC) are computed on top of OEPx orbitals.

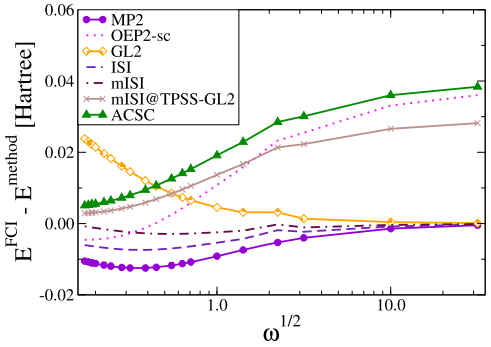

Figure 3. Absolute error on total energies of harmonium atoms for various values of ω.

To better see the functional performance at the strong-correlation limit ($\omega \to 0$), we report in Figure 4 the relative errors (RE) on the correlation energy. When $\omega \to 0$, mISI is the most accurate method being in good agreement with the ISI method computed with exact W_∞ and W'_∞.[62] On the other hand, the original ISI, which uses the PC model, gives quite large errors of about 30%, but still much better than GL2, which fails badly, with an error of about 120%. Note that when $\omega \to 0$, the density varies rapidly almost everywhere such that the reduced density gradient s is large, and the gradient expansion of the PC model cannot describe this regime.

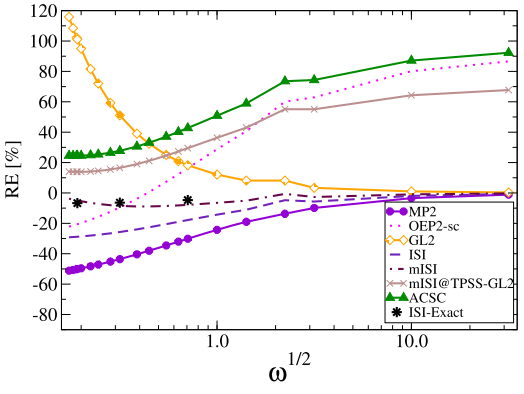

Figure 4. Relative error on correlation energies of harmonium atoms for various values of ω. The black dots (denoted with ISI-Exact) show the results of the ISI method computed with exact W_∞ and W'_∞, taken from ref 62.

4.4. Analysis of Functional Derivatives of W_∞ and W'_∞. Finally, in Figures 5 and 6, we report the comparison of the functional derivatives of W_∞^{PC} and $W_\infty'^{PC}$ and their modified counterparts for two representative systems, namely, H^- ion and N_2 molecule.

Let us turn first our attention to the H^- ion. We note that both mPC and PC W_∞ and W'_∞ potentials, like any other GGA, diverge on the nuclei, contrary to the exact SCE potential. Furthermore, in the tail of the density, both PC potentials diverge.[60] This is not the case for mPC potentials where we observe smooth and fast decay to zero in this region. We recall here that the exact SCE potential decays as $-1/r$ in the tail of the density. On the other hand, it was shown recently[117] that the functional derivative of an exact W'_∞ diverges in the tail for one-dimensional systems. This might indicate that the divergence is an exact feature of W'_∞ and $W_\infty'^{PC}$ is a more accurate model.

A similar behavior is observed for the N_2 molecule. In the nuclei, both potentials diverge, whereas in the far asymptotic region, the mPC potentials decay quite fast to zero in contrast to the PC potential which diverges.

We note, however, that the utilization of ISI-like functionals in practical KS calculations requires that the functional derivative of the XC functional is finite in the tail. Thus, one needs to remove the divergences of the functional derivative[118] despite whether this is an exact or model feature. This step is important toward the fully self-consistent implementation of ISI functionals.[118]

https://dx.doi.org/10.1021/acs.jctc.0c00328
J. Chem. Theory Comput. 2020, 16, 4983−4992

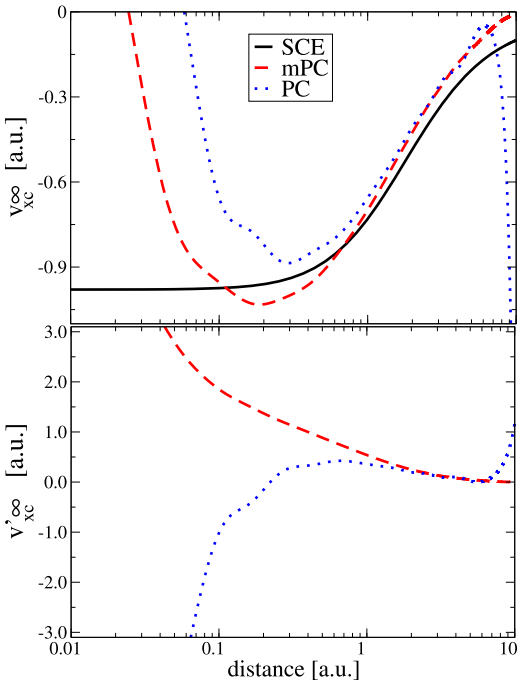

Figure 5. (Top) Comparison between the exact (SCE) functional derivative of W_∞ and the one computed from PC and modified PC model. (Bottom) Functional derivative of W'_∞ computed from PC and modified PC model. Both figures are done for H^-.

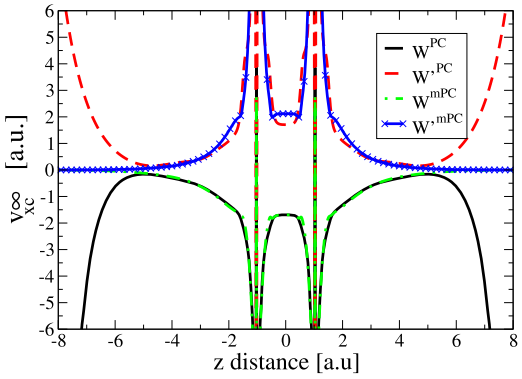

Figure 6. Functional derivative of PC and modified PC for N_2 molecule plotted along the bond axis.

5. CONCLUSIONS

We have presented a small assessment and comparison of ISI and mISI methods showing that the utilization of the modified PC model in ISI formula leads always to the improvement in the results. Moreover, the inspection of functional derivatives of W_∞ and W'_∞ obtained from the mPC model shows a lack of divergence in the tail of the density, which is a crucial step toward the self-consistent implementation of ISI functionals.

We note that the overall accuracy of the results provided by all ISI-like functionals is not better than other semilocal, hybrid, and double-hybrid functionals.[58] This is due to the dominant role of the GL2 or MP2 (depending on the reference orbitals used in the evaluation of energy) term in the ISI formula[60] for most of the chemically important applications. Thus, one possible way to improve the results is to include more terms in eq 3, *i.e.*, third-order GL/MP or higher. This, however, will significantly increase the cost of the method. Another possible path is to substitute the GL2/MP2 term by rescaled GL2/MP2[76] or one of spin-component-scaled variant[80,119−122] of GL or MP perturbation theory.

Finally, we mention that the mPC, and implicitly the mISI method, can be further improved by considering the Pauli kinetic energy enhancement factor[123−128] as an additional ingredient, which is relevant for one- and two-electron systems,[129] atomic core,[129] asymptotic behavior in the tail of the density,[130] and superior overall performance.[128] These will be a subject of further studies.

ASSOCIATED CONTENT

Supporting Information

The Supporting Information is available free of charge at https://pubs.acs.org/doi/10.1021/acs.jctc.0c00328.

Full results for Tables 1 and 2 with accompanying statistical analysis (Tables S1−S13) (PDF)

AUTHOR INFORMATION

Corresponding Author

Szymon Śmiga − *Institute of Physics, Faculty of Physics, Astronomy and Informatics, Nicolaus Copernicus University, 87-100 Toruń, Poland;* orcid.org/0000-0002-5941-5409; Email: szsmiga@fizyka.umk.pl

Author

Lucian A. Constantin − *Consiglio Nazionale delle Ricerche CNR-NANO, Istituto di Nanoscienze, 41125 Modena, Italy;* orcid.org/0000-0001-8923-3203

Complete contact information is available at: https://pubs.acs.org/10.1021/acs.jctc.0c00328

Notes

The authors declare no competing financial interest.

ACKNOWLEDGMENTS

S.Ś. is thankful to the Polish National Science Center (Grant No. 2016/21/D/ST4/00903) and CANALETTO Project (Nos. PPN/BIL/2018/2/00004 and PO19MO06) for partial financial support.

REFERENCES

(1) Langreth, D. C.; Perdew, J. P. The exchange-correlation energy of a metallic surface. *Solid State Commun.* **1975**, *17*, 1425−1429.

(2) Gunnarsson, O.; Lundqvist, B. I. Exchange and correlation in atoms, molecules, and solids by the spin-density-functional formalism. *Phys. Rev. B* **1976**, *13*, No. 4274.

(3) Savin, A.; Colonna, F.; Pollet, R. Adiabatic connection approach to density functional theory of electronic systems. *Int. J. Quantum Chem.* **2003**, *93*, 166−190.

(4) Cohen, A. J.; Mori-Sánchez, P.; Yang, W. Assessment and formal properties of exchange-correlation functionals constructed from the adiabatic connection. *J. Chem. Phys.* **2007**, *127*, No. 034101.

(5) Ernzerhof, M. Construction of the adiabatic connection. *Chem. Phys. Lett.* **1996**, *263*, 499−506.

(6) Burke, K.; Ernzerhof, M.; Perdew, J. P. The adiabatic connection method: a non-empirical hybrid. *Chem. Phys. Lett.* **1997**, *265*, 115−120.

(7) Colonna, F.; Savin, A. Correlation energies for some two-and four-electron systems along the adiabatic connection in density functional theory. *J. Chem. Phys.* **1999**, *110*, 2828−2835.

(8) Kohn, W.; Becke, A. D.; Parr, R. G. Density functional theory of electronic structure. *J. Phys. Chem. A* **1996**, *100*, 12974−12980.

(9) Becke, A. D. Density-functional thermochemistry. III. The role of exact exchange. *J. Chem. Phys.* **1993**, *98*, 5648−5652.

(10) Adamo, C.; Barone, V. Exchange functionals with improved long-range behavior and adiabatic connection methods without adjustable parameters: The m PW and m PW1PW models. *J. Chem. Phys.* **1998**, *108*, 664−675.
(11) Perdew, J. P.; Ernzerhof, M.; Burke, K. Rationale for mixing exact exchange with density functional approximations. *J. Chem. Phys.* **1996**, *105*, 9982−9985.
(12) Görling, A.; Levy, M. Exact Kohn-Sham scheme based on perturbation theory. *Phys. Rev. A* **1994**, *50*, No. 196.
(13) Görling, A.; Levy, M. Correlation-energy functional and its high-density limit obtained from a coupling-constant perturbation expansion. *Phys. Rev. B* **1993**, *47*, No. 13105.
(14) Görling, A.; Levy, M. Hardness of molecules and the band gap of solids within the Kohn-Sham formalism: A perturbation-scaling approach. *Phys. Rev. A* **1995**, *52*, No. 4493.
(15) Grimme, S. Semiempirical hybrid density functional with perturbative second-order correlation. *J. Chem. Phys.* **2006**, *124*, No. 034108.
(16) Møller, C.; Plesset, M. S. Note on an approximate treatment for many-electron systems. *Phys. Rev.* **1934**, *36*, 618−622.
(17) Grimme, S.; Neese, F. Double-hybrid density functional theory for excited electronic states of molecules. *J. Chem. Phys.* **2007**, *127*, No. 154116.
(18) Hui, K.; Chai, J.-D. SCAN-based hybrid and double-hybrid density functionals from models without fitted parameters. *J. Chem. Phys.* **2016**, *144*, No. 044114.
(19) Brémond, É.; Sancho-Garcia, J. C.; Perez-Jimenez, A. J.; Adamo, C. Communication: Double-hybrid functionals from adiabatic-connection: The QIDH model. *J. Chem. Phys.* **2014**, *141*, No. 031101.
(20) Sharkas, K.; Toulouse, J.; Savin, A. Double-hybrid density-functional theory made rigorous. *J. Chem. Phys.* **2011**, *134*, No. 064113.
(21) Souvi, S. M.; Sharkas, K.; Toulouse, J. Double-hybrid density-functional theory with meta-generalized-gradient approximations. *J. Chem. Phys.* **2014**, *140*, No. 084107.
(22) Goerigk, L.; Hansen, A.; Bauer, C.; Ehrlich, S.; Najibi, A.; Grimme, S. A look at the density functional theory zoo with the advanced GMTKN55 database for general main group thermochemistry, kinetics and noncovalent interactions. *Phys. Chem. Chem. Phys.* **2017**, *19*, 32184−32215.
(23) Cornaton, Y.; Franck, O.; Teale, A. M.; Fromager, E. Analysis of double-hybrid density functionals along the adiabatic connection. *Mol. Phys.* **2013**, *111*, 1275−1294.
(24) Kohn, W.; Sham, L. J. Self-consistent equations including exchange and correlation effects. *Phys. Rev.* **1965**, *140*, No. A1133.
(25) Seidl, A.; Görling, A.; Vogl, P.; Majewski, J. A.; Levy, M. Generalized Kohn-Sham schemes and the band-gap problem. *Phys. Rev. B* **1996**, *53*, 3764−3774.
(26) Śmiga, S.; Franck, O.; Mussard, B.; Buksztel, A.; Grabowski, I.; Luppi, E.; Toulouse, J. Self-consistent double-hybrid density-functional theory using the optimized-effective-potential method. *J. Chem. Phys.* **2016**, *145*, No. 144102.
(27) Sharp, R. T.; Horton, G. K. A Variational Approach to the Unipotential Many-Electron Problem. *Phys. Rev.* **1953**, *90*, 317.
(28) Talman, J. D.; Shadwick, W. F. Optimized effective atomic central potential. *Phys. Rev. A* **1976**, *14*, 36−40.
(29) Śmiga, S.; Grabowski, I.; Witkowski, M.; Mussard, B.; Toulouse, J. Self-Consistent Range-Separated Density-Functional Theory with Second-Order Perturbative Correction via the Optimized-Effective-Potential Method. *J. Chem. Theory Comput.* **2020**, *16*, 211−223. PMID: 31816237.
(30) Dobson, J. F.; Wang, J.; Gould, T. Correlation energies of inhomogeneous many-electron systems. *Phys. Rev. B* **2002**, *66*, No. 081108.
(31) Constantin, L. A.; Pitarke, J. M. Adiabatic-connection-fluctuation-dissipation approach to long-range behavior of exchange-correlation energy at metal surfaces: A numerical study for jellium slabs. *Phys. Rev. B* **2011**, *83*, No. 075116.
(32) Terentjev, A. V.; Constantin, L. A.; Pitarke, J. M. Gradient-dependent exchange-correlation kernel for materials optical properties. *Phys. Rev. B* **2018**, *98*, No. 085123.
(33) Constantin, L. A. Simple effective interaction for dimensional crossover. *Phys. Rev. B* **2016**, *93*, No. 121104.
(34) Corradini, M.; Del Sole, R.; Onida, G.; Palummo, M. Analytical expressions for the local-field factor G (q) and the exchange-correlation kernel K xc (r) of the homogeneous electron gas. *Phys. Rev. B* **1998**, *57*, No. 14569.
(35) Toulouse, J. Simple model of the static exchange-correlation kernel of a uniform electron gas with long-range electron-electron interaction. *Phys. Rev. B* **2005**, *72*, No. 035117.
(36) Richardson, C. F.; Ashcroft, N. W. Dynamical local-field factors and effective interactions in the three-dimensional electron liquid. *Phys. Rev. B* **1994**, *50*, No. 8170.
(37) Bates, J. E.; Laricchia, S.; Ruzsinszky, A. Nonlocal energy-optimized kernel: Recovering second-order exchange in the homogeneous electron gas. *Phys. Rev. B* **2016**, *93*, No. 045119.
(38) Bates, J. E.; Sensenig, J.; Ruzsinszky, A. Convergence behavior of the random phase approximation renormalized correlation energy. *Phys. Rev. B* **2017**, *95*, No. 195158.
(39) Ruzsinszky, A.; Constantin, L. A.; Pitarke, J. M. Kernel-corrected random-phase approximation for the uniform electron gas and jellium surface energy. *Phys. Rev. B* **2016**, *94*, No. 165155.
(40) Dobson, J. F.; Wang, J. Energy-optimized local exchange-correlation kernel for the electron gas: Application to van der Waals forces. *Phys. Rev. B* **2000**, *62*, No. 10038.
(41) Görling, A. Exact exchange kernel for time-dependent density-functional theory. *Int. J. Quantum Chem.* **1998**, *69*, 265−277.
(42) Kim, Y.-H.; Görling, A. Excitonic optical spectrum of semiconductors obtained by time-dependent density-functional theory with the exact-exchange kernel. *Phys. Rev. Lett.* **2002**, *89*, No. 096402.
(43) Erhard, J.; Bleiziffer, P.; Görling, A. Power Series Approximation for the Correlation Kernel Leading to Kohn-Sham Methods Combining Accuracy, Computational Efficiency, and General Applicability. *Phys. Rev. Lett.* **2016**, *117*, No. 143002.
(44) Patrick, C. E.; Thygesen, K. S. Adiabatic-connection fluctuation-dissipation DFT for the structural properties of solidsThe renormalized ALDA and electron gas kernels. *J. Chem. Phys.* **2015**, *143*, No. 102802.
(45) Görling, A. Hierarchies of methods towards the exact Kohn-Sham correlation energy based on the adiabatic-connection fluctuation-dissipation theorem. *Phys. Rev. B* **2019**, *99*, No. 235120.
(46) Seidl, M.; Perdew, J. P.; Kurth, S. Simulation of all-order density-functional perturbation theory, using the second order and the strong-correlation limit. *Phys. Rev. Lett.* **2000**, *84*, No. 5070.
(47) Seidl, M.; Perdew, J. P.; Kurth, S. Density functionals for the strong-interaction limit. *Phys. Rev. A* **2000**, *62*, No. 012502.
(48) Perdew, J. P.; Kurth, S.; Seidl, M. Exploring the adiabatic connection between weak-and strong-interaction limits in density functional theory. *Int. J. Mod. Phys. B* **2001**, *15*, 1672−1683.
(49) Gori-Giorgi, P.; Vignale, G.; Seidl, M. Electronic zero-point oscillations in the strong-interaction limit of density functional theory. *J. Chem. Theory Comput.* **2009**, *5*, 743−753.
(50) Liu, Z.-F.; Burke, K. Adiabatic connection in the low-density limit. *Phys. Rev. A* **2009**, *79*, No. 064503.
(51) Liu, Z.-F.; Burke, K. Adiabatic connection for strictly correlated electrons. *J. Chem. Phys.* **2009**, *131*, No. 124124.
(52) Magyar, R.; Terilla, W.; Burke, K. Accurate adiabatic connection curve beyond the physical interaction strength. *J. Chem. Phys.* **2003**, *119*, 696−700.
(53) Sun, J. Extension to Negative Values of the Coupling Constant of Adiabatic Connection for Interaction-Strength Interpolation. *J. Chem. Theory Comput.* **2009**, *5*, 708−711.
(54) Seidl, M.; Gori-Giorgi, P. Adiabatic connection at negative coupling strengths. *Phys. Rev. A* **2010**, *81*, No. 012508.

https://dx.doi.org/10.1021/acs.jctc.0c00328
J. Chem. Theory Comput. 2020, 16, 4983−4992

(55) Mirtschink, A.; Seidl, M.; Gori-Giorgi, P. Energy densities in the strong-interaction limit of density functional theory. *J. Chem. Theory Comput.* **2012**, *8*, 3097−3107.
(56) Gori-Giorgi, P.; Seidl, M. Density functional theory for strongly-interacting electrons: perspectives for physics and chemistry. *Phys. Chem. Chem. Phys.* **2010**, *12*, 14405−14419.
(57) Vuckovic, S.; Irons, T. J.; Savin, A.; Teale, A. M.; Gori-Giorgi, P. Exchange-correlation functionals via local interpolation along the adiabatic connection. *J. Chem. Theory Comput.* **2016**, *12*, 2598−2610.
(58) Fabiano, E.; Gori-Giorgi, P.; Seidl, M.; Della Sala, F. Interaction-strength interpolation method for main-group chemistry: benchmarking, limitations, and perspectives. *J. Chem. Theory Comput.* **2016**, *12*, 4885−4896.
(59) Giarrusso, S.; Gori-Giorgi, P.; Della Sala, F.; Fabiano, E. Assessment of interaction-strength interpolation formulas for gold and silver clusters. *J. Chem. Phys.* **2018**, *148*, No. 134106.
(60) Fabiano, E.; Śmiga, S.; Giarrusso, S.; Daas, T. J.; Della Sala, F.; Grabowski, I.; Gori-Giorgi, P. Investigation of the Exchange-Correlation Potentials of Functionals Based on the Adiabatic Connection Interpolation. *J. Chem. Theory Comput.* **2019**, *15*, 1006−1015.
(61) Vuckovic, S.; Gori-Giorgi, P.; Della Sala, F.; Fabiano, E. Restoring size consistency of approximate functionals constructed from the adiabatic connection. *J. Phys. Chem. Lett.* **2018**, *9*, 3137.
(62) Kooi, D. P.; Gori-Giorgi, P. Local and global interpolations along the adiabatic connection of DFT: a study at different correlation regimes. *Theor. Chem. Acc.* **2018**, *137*, No. 166.
(63) Zhou, Y.; Bahmann, H.; Ernzerhof, M. Construction of exchange-correlation functionals through interpolation between the non-interacting and the strong-correlation limit. *J. Chem. Phys.* **2015**, *143*, No. 124103.
(64) Seidl, M.; Giarrusso, S.; Vuckovic, S.; Fabiano, E.; Gori-Giorgi, P. Communication: Strong-interaction limit of an adiabatic connection in Hartree-Fock theory. *J. Chem. Phys.* **2018**, *149*, No. 241101.
(65) Constantin, L. A. Correlation energy functionals from adiabatic connection formalism. *Phys. Rev. B* **2019**, *99*, No. 085117.
(66) Vuckovic, S.; Irons, T. J.; Wagner, L. O.; Teale, A. M.; Gori-Giorgi, P. Interpolated energy densities, correlation indicators and lower bounds from approximations to the strong coupling limit of DFT. *Phys. Chem. Chem. Phys.* **2017**, *19*, 6169−6183.
(67) Vuckovic, S.; Gori-Giorgi, P. Simple Fully Nonlocal Density Functionals for Electronic Repulsion Energy. *J. Phys. Chem. Lett.* **2017**, *8*, 2799−2805.
(68) Perdew, J. P.; Staroverov, V. N.; Tao, J.; Scuseria, G. E. Density functional with full exact exchange, balanced nonlocality of correlation, and constraint satisfaction. *Phys. Rev. A* **2008**, *78*, No. 052513.
(69) Śmiga, S.; Constantin, L. A. Unveiling the Physics behind Hybrid Functionals. *J. Phys. Chem. A* **2020**, PMID: 32551627.
(70) Śmiga, S.; Constantin, L. A. Supporting Information.
(71) Perdew, J. P.; Kurth, S.; Zupan, A.; Blaha, P. Accurate density functional with correct formal properties: A step beyond the generalized gradient approximation. *Phys. Rev. Lett.* **1999**, *82*, No. 2544.
(72) Constantin, L. A.; Terentjevs, A.; Della Sala, F.; Fabiano, E. Gradient-dependent upper bound for the exchange-correlation energy and application to density functional theory. *Phys. Rev. B* **2015**, *91*, No. 041120.
(73) Lewin, M.; Lieb, E. H. Improved Lieb-Oxford exchange-correlation inequality with a gradient correction. *Phys. Rev. A* **2015**, *91*, No. 022507.
(74) Tao, J.; Staroverov, V. N.; Scuseria, G. E.; Perdew, J. P. Exact-exchange energy density in the gauge of a semilocal density-functional approximation. *Phys. Rev. A* **2008**, *77*, No. 012509.
(75) Perdew, J. P.; Burke, K.; Ernzerhof, M. Generalized gradient approximation made simple. *Phys. Rev. Lett.* **1996**, *77*, No. 3865.
(76) Śmiga, S.; Fabiano, E. Approximate solution of coupled cluster equations: application to the coupled cluster doubles method and non-covalent interacting systems. *Phys. Chem. Chem. Phys.* **2017**, *19*, 30249−30260.
(77) Stanton, J. F. et al. *ACES II*; Quantum Theory Project: Gainesville, Florida, 2007.
(78) Grabowski, I.; Teale, A. M.; Śmiga, S.; Bartlett, R. J. Comparing ab initio density-functional and wave function theories: The impact of correlation on the electronic density and the role of the correlation potential. *J. Chem. Phys.* **2011**, *135*, No. 114111.
(79) Śmiga, S.; Della Sala, F.; Buksztel, A.; Grabowski, I.; Fabiano, E. Accurate Kohn-Sham ionization potentials from scaled-opposite-spin second-order optimized effective potential methods. *J. Comput. Chem.* **2016**, *37*, 2081−2090.
(80) Grabowski, I.; Fabiano, E.; Teale, A. M.; Śmiga, S.; Buksztel, A.; Della Sala, F. D. Orbital-dependent second-order scaled-opposite-spin correlation functionals in the optimized effective potential method. *J. Chem. Phys.* **2014**, *141*, No. 024113.
(81) Śmiga, S.; Marusiak, V.; Grabowski, I.; Fabiano, E. The ab initio density functional theory applied for spin-polarized calculations. *J. Chem. Phys.* **2020**, *152*, No. 054109.
(82) Görling, A. New KS method for molecules based on an exchange charge density generating the exact local KS exchange potential. *Phys. Rev. Lett.* **1999**, *83*, 5459−5462.
(83) Ivanov, S.; Hirata, S.; Bartlett, R. J. Exact exchange treatment for molecules in finite-basis-set Kohn-Sham theory. *Phys. Rev. Lett.* **1999**, *83*, 5455−5458.
(84) Grabowski, I.; Teale, A. M.; Fabiano, E.; Smiga, S.; Buksztel, A.; Della Sala, F. D. A density difference based analysis of orbital-dependent exchange-correlation functionals. *Mol. Phys.* **2014**, *112*, 700−710.
(85) Mori-Sánchez, P.; Wu, Q.; Yang, W. Orbital-dependent correlation energy in density-functional theory based on a second-order perturbation approach: Success and failure. *J. Chem. Phys.* **2005**, *123*, No. 062204.
(86) Jiang, H.; Engel, E. Second-order Kohn-Sham perturbation theory: Correlation potential for atoms in a cavity. *J. Chem. Phys.* **2005**, *123*, No. 224102.
(87) Raghavachari, K.; Trucks, G. W.; Pople, J. A.; Head-Gordon, M. A fifth-order perturbation comparison of electron correlation theories. *Chem. Phys. Lett.* **1989**, *157*, 479−483.
(88) Bartlett, R. J.; Grabowski, I.; Hirata, S.; Ivanov, S. The exchange-correlation potential in ab initio density functional theory. *J. Chem. Phys.* **2005**, *122*, No. 034104.
(89) Curtiss, L. A.; Raghavachari, K.; Redfern, P. C.; Pople, J. A. Assessment of Gaussian-2 and density functional theories for the computation of enthalpies of formation. *J. Chem. Phys.* **1997**, *106*, 1063−1079.
(90) Lynch, B. J.; Truhlar, D. G. Small representative benchmarks for thermochemical calculations. *J. Phys. Chem. A* **2003**, *107*, 8996−8999.
(91) Haunschild, R.; Klopper, W. Theoretical reference values for the AE6 and BH6 test sets from explicitly correlated coupled-cluster theory. *Theor. Chem. Acc.* **2012**, *131*, No. 1112.
(92) Tentscher, P. R.; Arey, J. S. Geometries and Vibrational Frequencies of Small Radicals: Performance of Coupled Cluster and More Approximate Methods. *J. Chem. Theory Comput.* **2012**, *8*, 2165−2179. PMID: 26593847.
(93) Lynch, B. J.; Truhlar, D. G. Robust and Affordable Multicoefficient Methods for Thermochemistry and Thermochemical Kinetics: The MCCM/3 Suite and SAC/3. *J. Phys. Chem. A* **2003**, *107*, 3898−3906.
(94) Soyda, E.; Bozkaya, U. Assessment of Orbital-Optimized MP2.5 for Thermochemistry and Kinetics: Dramatic Failures of Standard Perturbation Theory Approaches for Aromatic Bond Dissociation Energies and Barrier Heights of Radical Reactions. *J. Chem. Theory Comput.* **2015**, *11*, 1564−1573. PMID: 26574366.
(95) Bozkaya, U.; Sherrill, C. D. Analytic energy gradients for the orbital-optimized second-order Møller-Plesset perturbation theory. *J. Chem. Phys.* **2013**, *138*, No. 184103.

https://dx.doi.org/10.1021/acs.jctc.0c00328
J. Chem. Theory Comput. 2020, 16, 4983−4992

(96) Dunning, T. H. Gaussian basis sets for use in correlated molecular calculations. I. The atoms boron through neon and hydrogen. *J. Chem. Phys.* **1989**, *90*, 1007−1023.
(97) Śmiga, S.; Grabowski, I. Spin-Component-Scaled ΔMP2 Parametrization: Toward a Simple and Reliable Method for Ionization Energies. *J. Chem. Theory Comput.* **2018**, *14*, 4780−4790. PMID: 30040889.
(98) Constantin, L. A.; Fabiano, E.; Śmiga, S.; Della Sala, F. Jellium-with-gap model applied to semilocal kinetic functionals. *Phys. Rev. B* **2017**, *95*, No. 115153.
(99) Śmiga, S.; Fabiano, E.; Constantin, L. A.; Della Sala, F. Laplacian-dependent models of the kinetic energy density: Applications in subsystem density functional theory with meta-generalized gradient approximation functionals. *J. Chem. Phys.* **2017**, *146*, No. 064105.
(100) Śmiga, S.; Fabiano, E.; Laricchia, S.; Constantin, L. A.; Della Sala, F. Subsystem density functional theory with meta-generalized gradient approximation exchange-correlation functionals. *J. Chem. Phys.* **2015**, *142*, No. 154121.
(101) Śmiga, S.; Constantin, L. A.; Della Sala, F.; Fabiano, E. The Role of the Reduced Laplacian Renormalization in the Kinetic Energy Functional Development. *Computation* **2019**, *7*, No. 65.
(102) Kendall, R. A.; Dunning, T. H., Jr.; Harrison, R. J. Electron affinities of the first row atoms revisited. Systematic basis sets and wave functions. *J. Chem. Phys.* **1992**, *96*, 6796−6806.
(103) Zhao, Y.; Truhlar, D. G. Design of Density Functionals That Are Broadly Accurate for Thermochemi stry, Thermochemical Kinetics, and Nonbonded Interactions. *J. Phys. Chem. A* **2005**, *109*, 5656−5667.
(104) Zhao, Y.; Truhlar, D. G. Benchmark Databases for Nonbonded Interactions and Their Use To Test Density Functional Theory. *J. Chem. Theory Comput.* **2005**, *1*, 415−432.
(105) Wesolowski, T. A.; Chermette, H.; Weber, J. Accuracy of approximate kinetic energy functionals in the model of Kohn-Sham equations with constrained electron density: The FH [center-dot] [center-dot] [center-dot] NCH complex as a test case. *J. Chem. Phys.* **1996**, *105*, 9182−9190.
(106) Fabiano, E.; Constantin, L. A.; Della Sala, F. Wave Function and Density Functional Theory Studies of Dihydrogen Complexes. *J. Chem. Theory Comput.* **2014**, *10*, 3151−3162.
(107) Kestner, N. R.; Sinanoğlu, O. Study of Electron Correlation in Helium-Like Systems Using an Exactly Soluble Model. *Phys. Rev.* **1962**, *128*, 2687−2692.
(108) Matito, E.; Cioslowski, J.; Vyboishchikov, S. F. Properties of harmonium atoms from FCI calculations: Calibration and benchmarks for the ground state of the two-electron species. *Phys. Chem. Chem. Phys.* **2010**, *12*, 6712−6716.
(109) Grabowski, I.; Lotrich, V. Accurate orbital-dependent correlation and exchange-correlation potentials from non-iterative ab initio dft calculations. *Mol. Phys.* **2005**, *103*, 2085−2092.
(110) Fabiano, E.; Della Sala, F. Localized exchange-correlation potential from second-order self-energy for accurate Kohn-Sham energy gap. *J. Chem. Phys.* **2007**, *126*, No. 214102.
(111) Śmiga, S.; Siecińska, S.; Fabiano, E. Methods to generate reference total and Pauli kinetic potentials. *Phys. Rev. B* **2020**, *101*, No. 165144.
(112) Taut, M. Two electrons in a homogeneous magnetic field: particular analytical solutions. *J. Phys. A: Math. Gen.* **1994**, *27*, 1045.
(113) Ludeña, E. V.; Gómez, D.; Karasiev, V.; Nieto, P. Exact analytic total energy functional for Hooke's atom generated by local-scaling transformations. *Int. J. Quantum Chem.* **2004**, *99*, 297−307.
(114) Amovilli, C.; March, N. Exact density matrix for a two-electron model atom and approximate proposals for realistic two-electron systems. *Phys. Rev. A* **2003**, *67*, No. 022509.
(115) O'Neill, D. P.; Gill, P. M. Wave functions and two-electron probability distributions of the Hooke's-law atom and helium. *Phys. Rev. A* **2003**, *68*, No. 022505.
(116) Das, G.; Wahl, A. C. Theoretical study of the F2 molecule using the method of optimized valence configurations. *J. Chem. Phys.* **1972**, *56*, 3532−3540.
(117) Grossi, J.; Seidl, M.; Gori-Giorgi, P.; Giesbertz, K. J. H. Functional derivative of the zero-point-energy functional from the strong-interaction limit of density-functional theory. *Phys. Rev. A* **2019**, *99*, No. 052504.
(118) Grossi, J.; Musslimani, Z. H.; Seidl, M.; Gori-Giorgi, P. Kohn-Sham Equations with Functionals from the Strictly-Correlated Regime: Investigation with a Spectral Renormalization Method. arXiv:2004.10436. arXiv.org e-Print archive. https://arxiv.org/abs/2004.10436 (submitted April 22, 2020).
(119) Grimme, S. Improved second-order Møller-Plesset perturbation theory by separate scaling of parallel- and antiparallel-spin pair correlation energies. *J. Chem. Phys.* **2003**, *118*, 9095−9102.
(120) Jung, Y.; Lochan, R. C.; Dutoi, A. D.; Head-Gordon, M. Scaled opposite-spin second order Møller-Plesset correlation energy: An economical electronic structure method. *J. Chem. Phys.* **2004**, *121*, 9793−9802.
(121) Witkowski, M.; Śmiga, S.; Grabowski, I. Density-Based Analysis of Spin-Resolved MP2 Method. In *Adv. Quantum Chem.*, Hoggan, P. E., Ed.; Novel Electronic Structure Theory: General Innovationsand Strongly Correlated Systems 1st Edition; Academic Press, 2018; Vol. *76*.
(122) Buksztel, A.; Śmiga, S.; Grabowski, I. Chapter Fourteen - The Correlation Effects in Density Functional Theory Along the Dissociation Path. In *Adv. Quantum Chem.*, Hoggan, P. E.; Ozdogan, T., Eds.; Electron Correlation in Molecules - Ab Initio Beyond Gaussian Quantum Chemistry; Academic Press, 2016; Vol. *73*, pp 263−283.
(123) Tao, J.; Perdew, J. P.; Staroverov, V. N.; Scuseria, G. E. Climbing the density functional ladder: Nonempirical meta-generalized gradient approximation designed for molecules and solids. *Phys. Rev. Lett.* **2003**, *91*, No. 146401.
(124) Sun, J.; Ruzsinszky, A.; Perdew, J. P. Strongly constrained and appropriately normed semilocal density functional. *Phys. Rev. Lett.* **2015**, *115*, No. 036402.
(125) Tao, J.; Mo, Y. Accurate semilocal density functional for condensed-matter physics and quantum chemistry. *Phys. Rev. Lett.* **2016**, *117*, No. 073001.
(126) Constantin, L. A.; Fabiano, E.; Della Sala, F. Semilocal Pauli-Gaussian kinetic functionals for orbital-free density functional theory calculations of solids. *J. Phys. Chem. Lett.* **2018**, *9*, 4385−4390.
(127) Constantin, L. A. Semilocal properties of the Pauli kinetic potential. *Phys. Rev. B* **2019**, *99*, No. 155137.
(128) Patra, B.; Jana, S.; Constantin, L. A.; Samal, P. Relevance of the Pauli kinetic energy density for semilocal functionals. *Phys. Rev. B* **2019**, *100*, No. 155140.
(129) Perdew, J. P.; Tao, J.; Staroverov, V. N.; Scuseria, G. E. Meta-generalized gradient approximation: Explanation of a realistic nonempirical density functional. *J. Chem. Phys.* **2004**, *120*, 6898−6911.
(130) Constantin, L. A.; Fabiano, E.; Pitarke, J. M.; Della Sala, F. Semilocal density functional theory with correct surface asymptotics. *Phys. Rev. B* **2016**, *93*, No. 115127.

https://dx.doi.org/10.1021/acs.jctc.0c00328
J. Chem. Theory Comput. 2020, 16, 4983−4992